$PbZrO_3$-Based Antiferroelectric Thin Film Capacitors with High Energy Storage Density

Mao Ye[1,2], Peng Lin[1], Haitao Huang[3], Biaolin Peng[1,2], Qiu Sun[4], Fuping Wang[4], Xiang Peng[2], Xierong Zeng[1,*] and Shanming Ke[1,*]

[1]*College of Materials Science and Engineering and Shenzhen Key Laboratory of Special Functional Materials, Shenzhen University, Shenzhen 518060, China*

[2]*College of Optoelectronic Engineering, Shenzhen University, Shenzhen 518060, China*

[3]*Department of Applied Physics and Materials Research Center, The Hong Kong Polytechnic University, Hung Hom, Kowloon, Hong Kong*

[4]*School of Chemical Engineering and Technology, Harbin Institute of Technology, Harbin 150001, China*

Abstract: A series of 400-nm-thick sandwich structured $Pb_{(1+x)}ZrO_3$/(Pb,Eu)ZrO_3/$Pb_{(1+x)}ZrO_3$(PZO/PEZO/PZO) antiferroelectric thin films with different Pb excess content (*x*) (*x*=0%, 10%, 20%, and 30%) in the PZO precursors have been successfully deposited on Pt(111)/Ti/SiO_2/Si substrates by a sol–gel method. The effects of Pb excess content on the dielectric properties, and energy storage performance of the PZO/PEZO/PZO thin films have been investigated in detail. It is found that all the films show a unique perovskite phase structure. With increasing Pb excess content in the PZO precursors, *P-E* hysteresis loop changes from slanted to square shape. Meanwhile, a larger antiferroelectric to ferroelectric switching field (E_{AF}) and ferroelectric to antiferroelectric switching field (E_{FA}) are observed in the films with higher Pb excess content. When increasing Pb excess content from 0% to 30%, the energy storage density of the sandwich structured films is remarkably improved from 11.4 to 14.8 J/cm^3 at 1000 kV/cm.

Keywords: Sandwich structure, Antiferroelectric, Thin films, Sol-gel, High energy density**.**

1. INTRODUCTION

Parallel plate capacitors with a high energy storage density are becoming increasingly important to a broad range of applications, especially in pulsed power circuit applications, such as hybrid electric vehicles (HEVs), medical devices, spacecraft, and electrical weapon systems [1-3]. In most of such devices, the capacitors take up a considerable percentage of volume and weight [4]. High energy density capacitors are the key components in these devices since they satisfy the general request for more compact devices and more functionalities can therefore be incorporated into these devices for a wider range of applications.

Theoretically, the accumulated electrostatic energy in a capacitor is stored in the dielectric material between the two parallel plates and is equal to the integral $U_e=\int EdP$, where E is applied electric field and P is the charge density (the polarization for ferroelectrics). Therefore, besides a high electric breakdown field E_b, a high P value is another key factor in achieving a high energy density. There are several classes of materials that can be considered for the development of high energy density capacitors, but each with its limitations. The energy densities for three kinds of materials are illustrated schematically as the shaded areas in Figure **1,** which are equal to the above mentioned integral. For linear dielectric materials, the energy density can be expressed as $U_e=1/2\varepsilon_r\varepsilon_0E^2$, where ε_r is relative dielectric constant, and ε_0 is the vacuum permittivity. Polypropylene (PC) is the most common linear dielectric for pulsed power application. Since it has a low dielectric constant (ε_r=2.2), it therefore has a low energy density of only 1-2 J/cm^3[5]. From Figure **1**, it can be seen that this low energy density is a result of the low polarization level in the dielectric material.

For ferroelectric (FE) material which has a high dielectric constant, however, the existence of a large remnant polarization (as shown in Figure **1b**) restricts the amount of stored electrostatic energy to be fully released. As shown in Figure **1c**, capacitors based on antiferroelectrics (AFE) offer dramatic improvement in energy density when compared to conventional ferroelectric capacitors. AFE materials are those that have spontaneous polarizations with adjacent dipoles being opposite, which can be aligned to a FE state by a threshold electric field (E_{AF}); the FE state can return to

*Address correspondence to these authors at the College of Materials Science and Engineering and Shenzhen Key Laboratory of Special Functional Materials, Shenzhen University, Shenzhen, China; Tel: +86 755 26534059; Fax: +86-755-26534457; E-mail: smke@szu.edu.cn and zengxier@szu.edu.cn

E-ISSN: 2408-977X/14

the AFE state when the field is decreased below a threshold electric field (E_{FA}) [6].

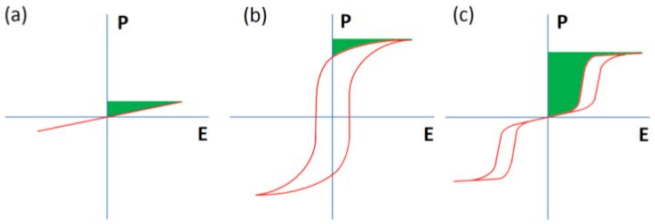

Figure 1: A schematic cartoon of *P-E* behavior of **(a)** linear, **(b)** ferroelectric (FE), and **(c)** antiferroelectric (AFE) materials. The shaded area of the polarization (*P*) and electric field (*E*) is related to the stored energy density of the dielectrics.

It is well known that $PbZrO_3$ (PZO) is the typical and one of the most widely studied AFE materials, whose energy storage density can reach a possibility of 50 J/cm^3 during the phase switching [7]. There are a lot of reports on energy storage for PZO-based materials, such as PLZO, PLZT, PLZST, and so on [8-12]. Based on these studies, it was concluded that the energy storage density can be improved by increase square ness of the *P-E* loop, applicable electric field, and phase switching field from FE to AFE. In our previous study, a high energy density of 18.8 J/cm^3 was achieved in Eu-dopedPZO (PEZO) thin film capacitors [13]. Eu-doped compositionally graded multilayer PZO thin films were also investigated thoroughly for energy storage [14]. In this paper, we present a preliminary study on the electrical properties of $Pb_{(1+x)}ZrO_3$/(Pb,Eu)ZrO_3/$Pb_{(1+x)}ZrO_3$ (PZO/PEZO/PZO) sandwich thin films. The films were deposited on Pt(111)/Ti/SiO_2/Si substrates by a sol-gel method. The final dielectric properties and energy storage performance of these thin films were investigated in detail as a function of Pb excess content in the PZO precursors.

2. EXPERIMENTAL DETAILS

Metal oxide precursors of 0.4 M concentration of 3 mol% Eu-doped PZO (20% excess Pb) and pure PZO (0% to 30% excess Pb) were prepared by a sol-gel process. The preparation method to obtain pure and Eu-doped PZO sol was similar to our earlier reports [13]. After aged 24h, the bottom PZO layer was coated on Pt(111)/Ti/SiO_2/Si (100) substrates via a multiple-spin-coating procedure. Each PZO layer was spin coated at 3000 rpm for 20s and pyrolyzed on a hot plate at 450^{o}C for 3min. After the deposition of a bottom PZO layer, PEZO layer and upper PZO layer were deposited by the same procedure. Finally, the films were annealed at 650^{o}C for 3min under oxygen atmospheric conditions by a rapid thermal annealing (RTA) process. Platinum top electrodes with 200μm diameter were deposited on the surface of these films by RF Magnetron Sputtering using a shadow mask. In this paper, we refer to the excess Pb based on the Pb in the PZO solution and not the final films. The films fabricated by using the solution with excess Pb of 0%–30% are denoted to be the 0%–30% films.

The phase structure of the films was examined using a Philips'X-ray diffraction (XRD) with Cu Kα radiation. Thickness and surface microstructures of the films were evaluated by using a scanning electron microscopy (SEM, JSM JEOL, Japan). The *P-E* hysteresis of the films has been measured by Radiant Premier II tester (Radiant Technologies, Inc.). The frequency dependent dielectric properties of the films were performed using animpedance analyzer (Solartron SI 1260, UK).

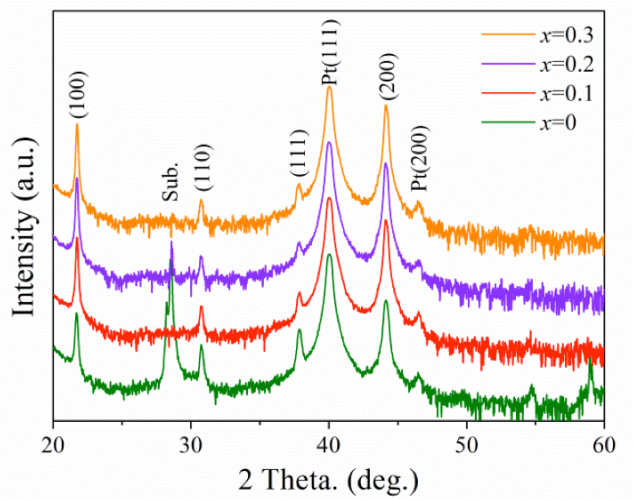

Figure 2: XRD patterns of the PZO/PEZO/PZO thin films with different Pb excess content (*x*) in the PZO precursors.

3. RESULTS AND DISCUSSIONS

Figure **2** presents X-ray diffraction patterns of the PZO/PEZO/PZO thin films grown on Pt bottom electro-des with an annealing temperature of 650^{o}C.The diffraction peaks of the XRD pattern can be indexed according to a pseudo-cubic structure. Clearly, all the sandwich films had crystallized into pure perovskite structure without any other phase. It is worthy to note that with the increase of Pb excess content in the PZO precursors, the peak intensity of (111) decreases while a very strong (100)-preferred orientation is obtained, which is very similar to other lead-based AFE and/or

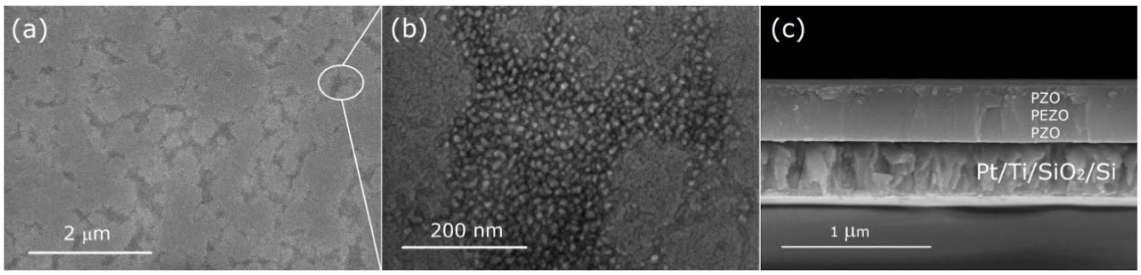

Figure 3: Typical surface **(a, b)** and cross-section SEM images of PZO/PEZO/PZO thin films with *x*=0.3**.**

FE films [13-15]. It is accepted that due to a higher lead excess in precursors, (100)-oriented PbO layer formed transiently on Pt surface and then induced the subsequent AFE films to grow along the orientation.

Figure **3(a, b)** displays surface SEM photographs of PZO/PEZO/PZO thin films with *x*=0.3. Clear rosette structure (round light-colored phase) is present in all films and neck is formed in-between the rosettes, which is a typical microstructure of lead-based FE/AFE thin films fabricated by chemical solution methods [16]. Energy dispersive spectroscopy results (not shown here) indicated that the rosettes phase (as shown in Figure **3a**) was rich in lead and the dark phase (as shown in Figure **3b**) was deficient in lead. Figure **3(c)** shows typical cross-section SEM image of PZO/PEZO/PZO thin films with *x*=0.3, which indicated that the films had a dense structure with a thicknesses of about 380 nm.

The frequency dependences of dielectric constant (*ε*) and dielectric loss (*tanδ*) are shown in Figure **4**, which were measured at room temperature and over 100Hz-1M Hz. The dielectric constant is slightly decreased with the increase of frequency indicating that the dielectric properties have not remarkable dispersion in the whole measured frequency range. Whereas the dielectric loss is increased obviously at higher frequency ranges. Moreover, Pb excess content has a strong influence on the dielectric constant of the PZO/PEZO/PZO thin films. It can be seen that the dielectric constant at 100kHz is 271, 219, 181, and 191 for films with Pb excess content of 0%, 10%, 20%, and 30%, respectively. All the films display small dielectric losses below 0.09, which could be attributed to their uniform microstructures. It's worthy to note that the dielectric constant of AFE materials has a close relationship with the stability of AFE state. Generally, higher stability of the AFE state usually leads to lower dielectric constant. The sandwich films with higher Pb excess content had lower dielectric constant, which increased the stability of AFE phase.

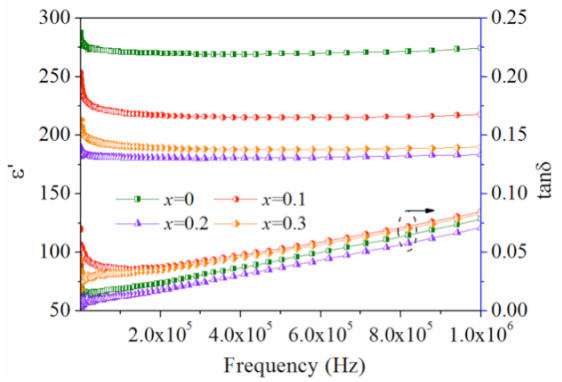

Figure 4: Frequency dependent dielectric constant and dielectric loss of the PZO/PEZO/PZO thin films with different Pbexcess content (*x*) in the PZO precursors.

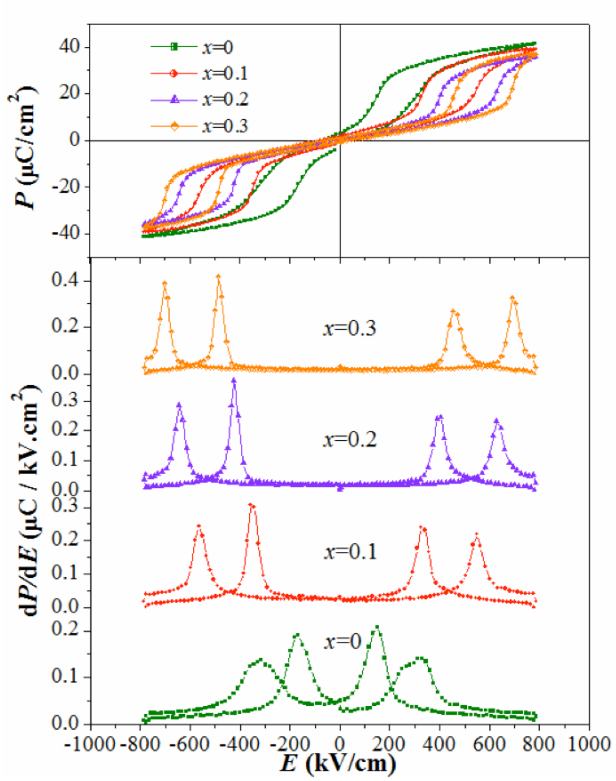

Figure 5 (a): P–E loops of the PZO/PEZ/PZO thin films with different Pb excess content (*x*) in the PZO precursors. **(b)** Differentiated *P-E* hysteresis loops of the PZO/PEZ/PZO thin films.

P-E loops of the PZO/PEZ/PZO thin films are shown in Figure **5(a).** All the samples show clearly double hysteresis loops, indicating that all the films are AFE materials. As Pb excess content in the PZO precursors is increased, saturation polarization decreases from 41 to 36 μC/cm^2, and on the extent of Pb content, the AFE-FE phase transition of the *P-E* hysteresis loop shows a rapid increase, indicating a change from diffused phase switching to sharp phase switching between AFE and FE phases. According to the earlier reports on AFE materials [17], square *P-E* loop is more efficient in energy storage devices than the slanted. Because the slope of *P-E* loop is relative with the dielectric constant of the films, this value can be expected to increase sharply as the sample through the AFE to FE and FE to AFE phase transition. From the differentiated *P-E* curves shown in Figure **5(b)**, films with higher Pb excess content in the PZO precursors show a larger E_{AF} and E_{FA}. The values of E_{AF} are 152, 327, 405, and 454kV/cm for the PZO/PEZO/PZO films with x from 0 to 0.3, respectively. The larger E_{AF} indicates better stability of the AFE phase, which is consistent with the dielectric constant results.

Figure **6(a)** depicts the change of maximum polarization (P_{max}) with respect to the maximum electric field. In all the cases, the P_{max} is constant with increasing the applied field, and the larger P_{max} is obtained at the higher electric field. It is important to note that the field dependence of the P_{max} can be separated into three distinct linear zones, including AFE region at lower applied field, AFE to FE transformation regions without saturation, and with saturation at higher field. Moreover, with increasing Pb excess content in the PZO precursors, the intersection point of AFE region and AFE to FE transformation region without saturation is shifted to higher field. It indicates that AFE state of the PZO/PEZO/PZO thin films is enlarged and stabilized by a higher Pb excess content. According to the definition of energy storage density, $U_e=\int EdP$, the function of electric field applied and energy storage density, energy loss (integral of the area enclosed by the *P-E* loop and *y*-axis) of the thin films with different Pbexcess content in the PZO precursors are calculated and given in Figures **6(b)** and **(c)**. In all films, the energy storage density and energy loss increase with increasing the electric field. At lower applied field, the energy density of all the films is small and increase slightly due to the absence of field induced AFE to FE transformation. The energy density increases rapidly within AFE–FE phase switching without saturation of polarization. At a higher electric field, the energy storage densities and energy loss of the PZO/PEZO/PZO thin films with Pb excessin the PZO precursors are elevated greatly, compared with those of the PZO/PEZO/PZO films with Pb excess content x=0%. As it is expected, at 1000 kV/cm, the energy storage densities are 11.2, 13.1, 14.4, and 14.8 J/cm^3, and the energy loss are 6.7, 8.9, 7.8, and 9.5 J/cm^3 for Pb excess content of 0%, 10%, 20%, and 30% in the PZO precursors, respectively. Moreover, with increasing Pb excess content in the PZO precursors, the films response changes from gradual to steep, which is in agreement with the change in shape of the *P-E* loops from slanted to square.

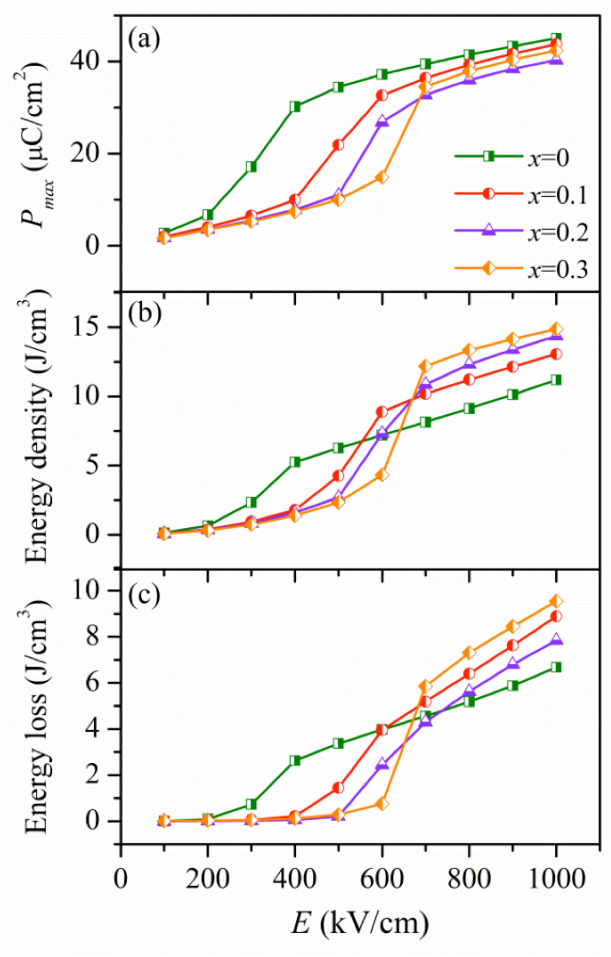

Figure 6 (a): Field dependent maximum polarization of the PZO/PEZO/PZO thin films with different Pb excess content (x) in the PZO precursors. **(b)** Energy density of the PZO/PEZO/PZO thin films under increasing electric field. **(c)** Energy loss observed in the PZO/PEZO/PZO thin films under elevated electric field.

4. CONCLUSIONS

In conclusion, sandwich structured PZO/PEZO/PZO films with a unique perovskite structures are obtained

by a sol–gel technique. Pb excess content in the PZO precursors has influences on the electrical properties, and energy storage performance of PZO/PEZO/PZO AFE thin films. With increasing Pb excess content in the PZO precursors, the shape of the *P-E* hysteresis loop becomes relatively more “square”, and the AFE state of PZO/PEZO/PZO thin films is enlarged and stabilized, which are more efficient in energy storage devices. Therefore, the energy storage performance of Pb-based sandwich structured films can be optimized by proper controlling Pb excess content in the buffer and surface layers.

ACKNOWLEDGEMENTS

This work was supported by the National Natural Science Foundations of China (Nos. 51302172 and 51272161).

REFERENCES

[1] Chu BJ, Zhou X, Ren KL, Neese B, Lin MR, Wang Q, *et al*., Science 2006; 313: 334-336.

[2] Cao Y, Irwin PC, Younsi K, IEEE T Dielect El In 2004; 11: 797-807.

[3] Wang Q, Zhu L, J PolymSci Part B: PolymPhys 2011; 49: 1421-1429.

[4] Karden E, Ploumen S, Fricke B, Miller T, Snyder K, J Power Sources 2007; 168: 2-11.

[5] Wisken HG, Weise THGG, IEEE T Magn 2003; 39: 501-504.

[6] Haertling GH, J Am Ceram Soc 1999; 82: 797-818.

[7] Sternberg A, Kundzinsa K, Zaulsa V, Aulikaa I, Akare LC, Bittnerc R, *et al*., J Eur Ceram Soc 2004; 24: 1653-1657.

[8] Mirshekarloo MS, Yao K, Sritharan T. ApplPhysLett 2010; 97: 142902.

[9] Xu ZK,Zhai JW, Chan WH, Chen H. ApplPhysLett 2006; 88:132908.

[10] Hao XH, Zhai JW, Yao X, J Am Ceram Soc 2009; 92: 1133-1135.

[11] Hao XH, Zhai JW, Kong LB, Xu ZK, Prog Mater Sci 2014; 63: 1-57.

[12] Ma BH, Kwon DK, Narayanan M, Balachandran UB, J Mater Res 2009; 24: 2993-2996.

[13] Ye M, Sun Q, Chen XQ, Jiang ZH, Wang FP, J Am Ceram Soc 2012; 95: 1486-1488.

[14] Ye M, Sun Q, Chen XQ, Jiang ZH, Wang FP, J Am Ceram Soc 2011; 94: 3234-3236.

[15] Gong W, Li JF, Chu XC, Gui ZL, Li LT, Acta Mater 2004; 52: 2787-2793.

[16] Xu BM, Cross LE, Ravichandran D, J Am Ceram Soc 1999; 82: 306-312.

[17] Hao XH, Zhou J, An SL. J Am Ceram Soc. 2011; 94: 1647-1649.

Received on 27-05-2014 Accepted on 31-05-2014 Published on 28-08-2014

http://dx.doi.org/10.15379/2408-977X.2014.01.01.4